JTTEE5 15:750-758
DOI: 10.1361/105996306X147036
1059-9630/$19.00 © ASM International

Peer Reviewed

# High-Speed Visualization and Plume Characterization of the Hybrid Spray Process

*J. Stanisic, D. Kosikowski, and P.S. Mohanty*

*(Submitted March 1, 2006; in revised form April 29, 2006)*

**The hybrid spray process that combines arc spray with a high-velocity oxyfuel (HVOF)/plasma jet has recently demonstrated its effectiveness in deposition of functionally gradient coatings. This approach aims at exploiting the combined attributes of the arc-spray technique and the HVOF/air plasma spraying (APS) technique. This paper presents high-speed visualization and plume characterization of an arc/HVOF hybrid spray gun as well as a twin-wire arc-spray gun. The physics of atomization in the hybrid spray process is examined using a high-speed camera. A DPV/CPS-2000 (Tecnar, St-Bruno, QC, Canada) particle diagnostics sensor is used to measure particle velocity, temperature, size, and distribution. The influence of feed material, arc parameters, and HVOF parameters on the particle characteristics is presented. Differences in the in-flight characteristics between the hybrid and the twin-wire arc process are discussed aided by the observed atomization phenomena with the high-speed camera.**

**Keywords** arc, diagnostics, HVOF, hybrid gun, visualization

## 1. Introduction

Many variants of thermal spraying technology exist. Among them, the high-velocity oxyfuel (HVOF) gun represents a major development. The HVOF gun results in hypersonic flame gas velocities, and powder particles attain high heat and high velocities. This permits particle flattening upon striking the substrate, thus forming a dense coating. HVOF-sprayed metallic coatings often have properties superior to those of plasma/arc-sprayed coatings.

The twin-wire arc-spray gun, on the other hand, is a widely used method for application of metallic coatings. The main attractions are its low cost and operational simplicity. During the process, an electric arc melts the wires and the molten metal is atomized by a continuous flow of either high-velocity compressed air or nonoxidizing gases, such as nitrogen or argon. Coatings formed using electric arc-spray guns are relatively less dense, but deposition rates are much higher compared with the HVOF process.

A recent development called "the hybrid process" (Ref 1, 2) combines electric arc and HVOF spraying; molten metal at the arc is atomized and rapidly propelled to the substrate by a HVOF jet (Fig. 1). This so-called "hybrid" concept aims at exploiting the benefits of both processes. The process offers all benefits of wire stock and productivity of electric arc spraying combined with noticeably improved coating density of HVOF. In addition to producing high-throughput dense coatings, the gun can also tailor the composition of the coating by introducing powder particles (e.g., carbide) through the HVOF jet in order to cater to specific property requirements, such as a functionally graded material (FGM).

The schematic arrangement of the hybrid gun is shown in Fig. 1. The HVOF component of the system combusts propylene/propane with oxygen and is air-cooled. The arc component is designed such that the relative distance between the HVOF nozzle and the arc strike point can be changed as well as the angle between the wires can be varied easily. The system is designed and developed in-house. With its flexible design, the hybrid gun can operate in three distinct modes: (I) partial-hybrid mode, where the material is introduced via arcing of wires only; the robustness of the hybrid gun allows it to be operated in two-wire arc or four-wire arc mode; (II) full-hybrid mode, where material is introduced through both arcing of wires and as a powder or wire through the HVOF feed line; and (III) HVOF mode, where material is fed as either a powder or a single wire to the HVOF gun. Because of the characteristic differences of the injected materials as well as the thermal energy utilization phenomena, the hybrid process involves extensive process parameters. Governing parameters, such as the arc power level, the flow parameters of the HVOF component, the powder injection and wire feed configurations, etc., involve so many possible combinations that design optimization is very complex. The multitude of interdependent process parameters results in a range of particle characteristics within the spray plume. The particle characteristics in turn determine the deposit build-up process and deposit properties (Ref 3). To make the process design and development robust, it is important that the correlation between the gun operating parameters and the resulting in-flight particle characteristics is well understood and predictable.

Spray plume characterization studies have become more common as particle diagnostics techniques have improved (Ref 4-29). Over the last two decades, many types of non-intrusive diagnostic instruments have been developed to measure particle

This article was originally published in *Building on 100 Years of Success, Proceedings of the 2006 International Thermal Spray Conference* (Seattle, WA), May 15-18, 2006, B.R. Marple, M.M. Hyland, Y.-Ch. Lau, R.S. Lima, and J. Voyer, Ed., ASM International, Materials Park, OH, 2006.

**J. Stanisic, D. Kosikowski,** and **P.S. Mohanty,** Additive Manufacturing Process Laboratory (AMPL), University of Michigan—Dearborn, 4901 Evergreen Road, Dearborn, MI 48188. Contact e-mail: pmohanty@umich.edu.

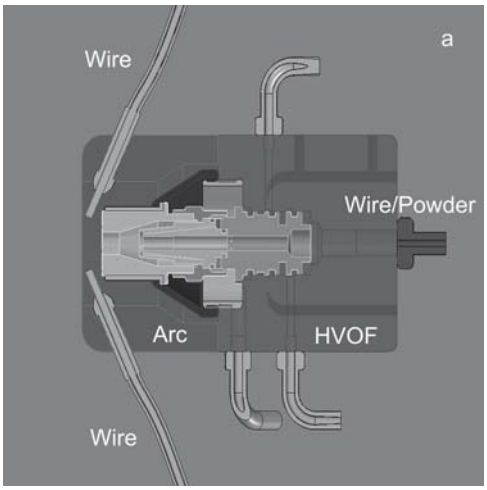


**Fig. 1** Schematic view of the arc/HVOF hybrid gun

characteristics in thermal spray plumes. These instruments have had significant roles in the advancement of thermal spray technology.

Particle temperature measurement usually relies on the ratio of the emitted radiance of hot, incandescent, particles in two or more wavelengths. Use of this ratio makes its unnecessary to perform an absolute intensity calibration. For lack of better information, the particles are generally assumed to behave as gray-body emitters. Measurement techniques fall into two categories: single particle and ensemble methods. Single-particle methods use high-speed pyrometry to estimate the temperature of individual particles. Ensemble methods observe large numbers of particles simultaneously and yield an estimated mean temperature directly. Both techniques and their inherent strengths and limitations are discussed in Ref 24.

The velocity of thermal spray particles has been measured using several techniques, including laser Doppler velocimetry (LDV; Ref 10), particle streak velocimetry (PSV; Ref 11), phase Doppler interferometry (PDI; Ref 19), and others (Ref 20). All particle velocity measurements currently available are single-particle techniques. However, new techniques that are based on the cross-correlation of signals from two closely spaced apertures provide an ensemble average particle velocity. Often in a spray plume, the particle temperature varies significantly. Cold particles with temperatures less than ~1000 °C cannot be detected without external illumination, such as a laser.

The objectives of this study are to explore the physics involved and to address qualitatively and quantitatively the ability of this system to atomize and deposit materials effectively. An in-depth plume characterization study on the hybrid gun as well as Tafa (Proxair Surface Technologies, Indianapolis, IN) Model 8830 twin-wire arc gun has been done using the DPV/CPS-2000 system (Tecnar, St-Bruno, QC, Canada). The influences of feed material, arc parameters, and HVOF parameters on the particle characteristics are presented. To substantiate the plume characterization measurements, high-speed visualization studies have been conducted using a high-speed camera (~100,000 frames/s, DS70K, Canadian Photonics Labs, Minnedosa, Manitoba, Canada) and various band-pass filters.

## 2. Experimental Procedures

As mentioned earlier, the hybrid gun can operate in various modes. This characterization study was conducted in three parts: (I) operation of gun in partial-hybrid mode using two-wire arcing, (II) in full-hybrid mode using two-wire arcing and powder through the HVOF feed line at different ratios while attempting to keep the overall mass flow constant, and (III) operation in HVOF mode with material fed in powder as well as wire form. Two material systems were considered in this study: (a) WC-16% $Cr_3C_2$-7% Ni (powder) and Ni-5% Al (wire) and (b) Al wire and Al powder. These materials were sprayed with propylene/oxygen as the HVOF fuel. The following parameters were varied to examine the interaction between the arc and the HVOF: (I) the included angle between arcing wires, set at 60, 90, 120, and 135°; (II) the distance between the HVOF nozzle and arcing point, set at 2, 4, 6, and 8 mm; and (III) HVOF gas pressures, varied from 20 to 50 psi for propylene, from 40 to 75 psi for oxygen, and from 50 to 90 psi for compressed air. The arcing parameters were set at 75 A and 30 V. Particle velocities, temperatures, and diameters were measured under these conditions at various distances from the gun tip using the DPV/CPS-2000 system. Plume cross-sectional contour maps at various distances from the gun tip were also compiled to study the atomization behavior of the hybrid gun. The DPV-2000 system makes possible on-line measurement of surface temperature, velocity, and diameter of individual particles in a spray plume by the principle of two-wavelength pyrometry (Ref 24, 26), with a sensor composed of a focusing lens and an optical fiber. A mask with two slits is fixed in front of the optical fiber. The signal emitted by a hot particle crossing the measuring volume is detected by the sensor located 10 cm from the plume. The two-peak signal due to the presence of the mask is filtered at two different wavelengths, amplified, and treated by a computer. The temperature is deduced from the signals of the two wavelengths assuming that the particle is a gray body. The diameter is calculated after calibration from the signal at one wavelength. The velocity is deduced from the time between the two peaks because the distance between the slits is known. The CPS-2000 system uses a diode laser to illuminate the cold particles for velocity measurement. Particle velocities were also measured by the high-speed camera using a superimposed background grid. By knowing the frame rate and magnification, one can measure the distance traveled by a particle in a given time. This data are computed by a computer program to calculate the average velocity. During high-speed photography, a HOYA r-72 filter (38% transmittance at 720 nm, up to 90% at 800 nm continuing to ~2000 nm) was used to suppress the arc emissions.

## 3. Results and Discussion

The in-flight particle data were acquired in different modes as described above. Only selected results are presented here. Figure 2 presents typical cross-sectional maps of particle velocity and flow rate in mode I operation. Because the wires are fed from the left and right, the gas flow is directed up and down from the arcing point. The influence of the obstruction provided by the arcing tip is distinctively seen on both the particle velocity and flow rate contour plots. The corresponding particle tempera-

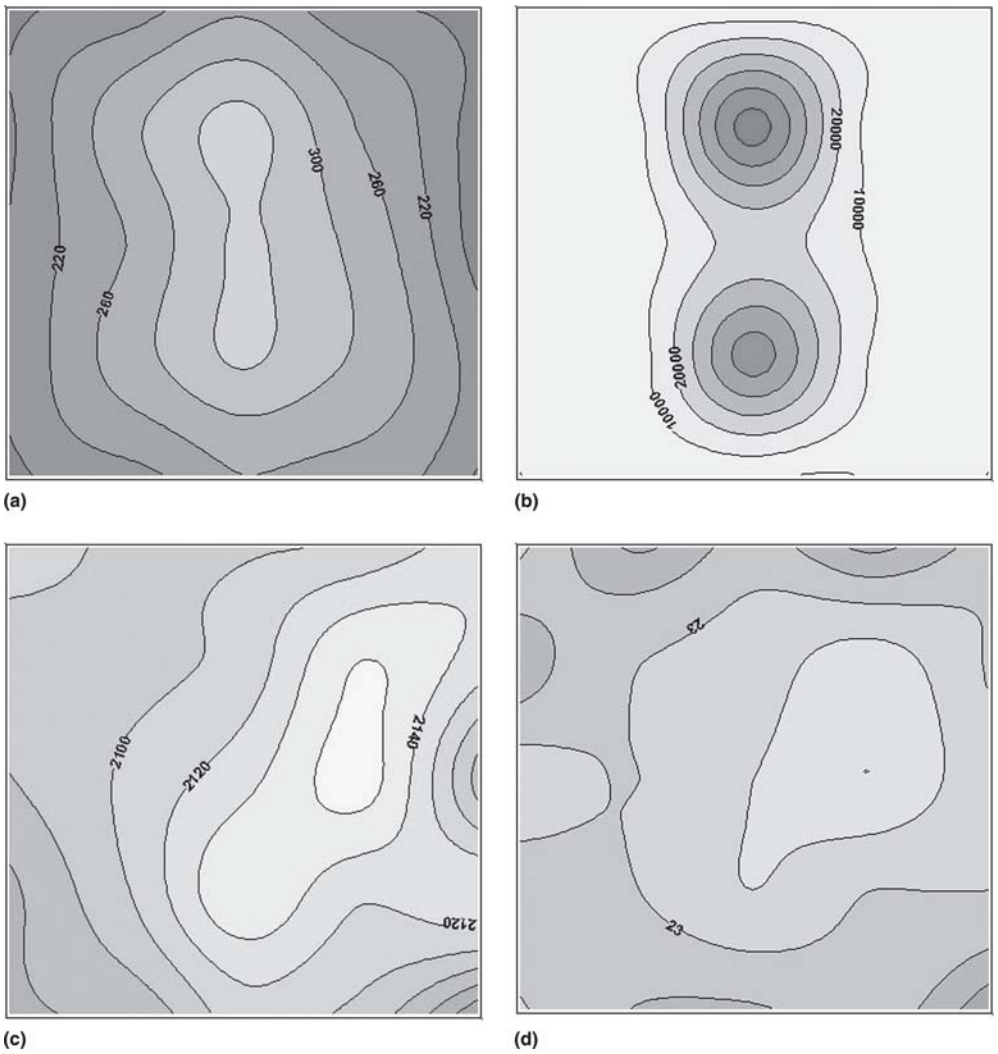


**Fig. 2** (a) Velocity (m/s), (b) particle flow rate, (c) temperature (°C), and (d) particle diameter (μ) contour plots in mode I (0% powder, 100% Ni-Al wire, 150 mm target distance)

ture and mean diameter plots show that particle temperature and mean diameter do not vary greatly through the slice of the plume.

Figure 3 illustrates the particle velocity and temperature measurements in mode I using Ni-5%Al wire at various distances from the gun tip (target distance). It was observed that, although the particle temperature remained relatively steady along the plume, the velocity rapidly increased then decreased. This behavior has been observed in twin-wire arc guns and is well known (Ref 17, 27). However, the magnitude of the average velocity was much higher (~300 m/s) than a conventional wire arc gun (~130 m/s).

The particle flow rate map in mode II with aluminum wire and the corresponding flow rate map in a twin-wire arc gun are presented in Fig. 4. The scan areas were kept constant (30 × 30 mm) for both the experiments. In the case of the hybrid gun, most of the particles were concentrated around a tight region, where as the scan area was sparsely populated in the case of twin-wire arc gun. The particle distribution in the plume has

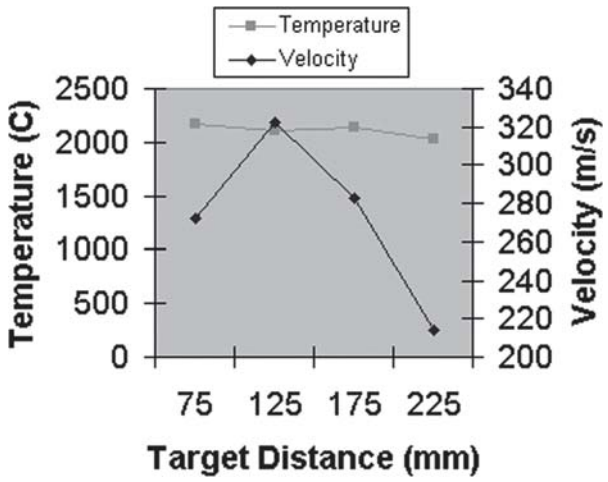


**Fig. 3** Velocity and temperature variation at different distances in mode I (0% powder, 100% Ni-Al wire)

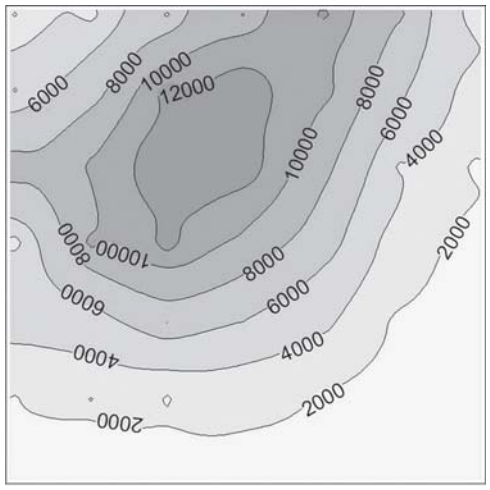


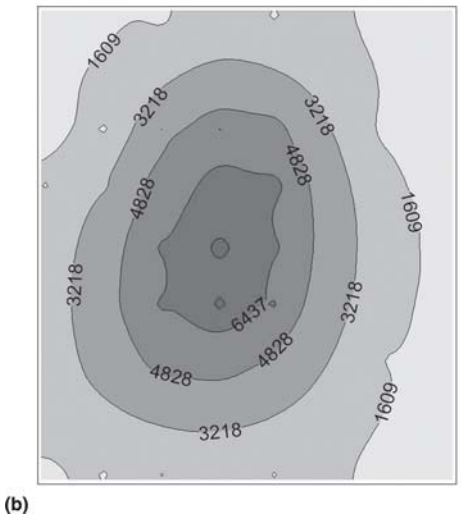


**Fig. 4** Particle flow rate contour plots: (a) hybrid gun in mode I and (b) twin-wire arc gun (100% Al wire, 150 mm target distance)

considerable significance in terms of the coating quality in addition to the observed velocity achieved in the hybrid gun.

In pure HVOF mode (mode III), the particle temperature also remained relatively steady along the plume, but the velocity continually decreased (Fig. 5). This is typical of commercial HVOF guns (Ref 26). Figure 6 shows the particle velocity and flow rate contour plots when the operation is switched from mode I to mode III while keeping the HVOF parameters identical. Although the plots are very similar in nature, the particle mean velocity was higher as expected and the plume was more contained. In mode III operation, the presence of the wire tips still influence the flow dynamics of the spray plume. Also, the particle flow rate was significantly lower because only powder material was fed. It is to be noted that, compared with the velocities achieved in commercial HVOF guns (~400-500 m/s; Ref 26), the particle velocity observed in the hybrid gun is lower. The HVOF component used herein is designed to operate at low combustion rates and is air-cooled, whereas commercial HVOF guns operate at high combustion rates and are water-cooled.

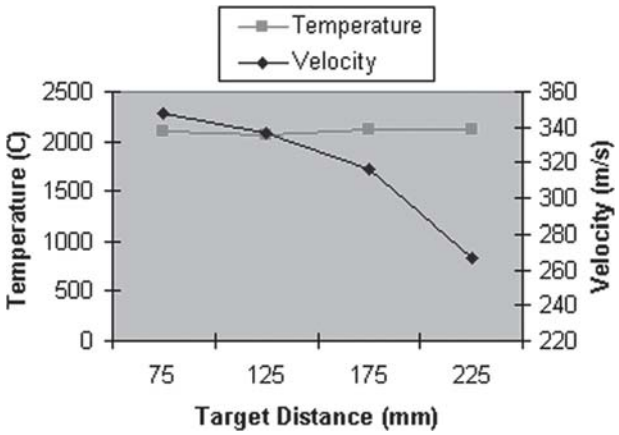


**Fig. 5** Velocity and temperature variation at different distances in mode III (100% powder, 0% wire)

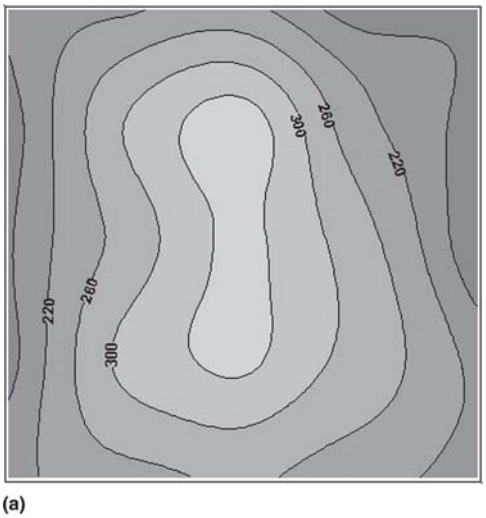


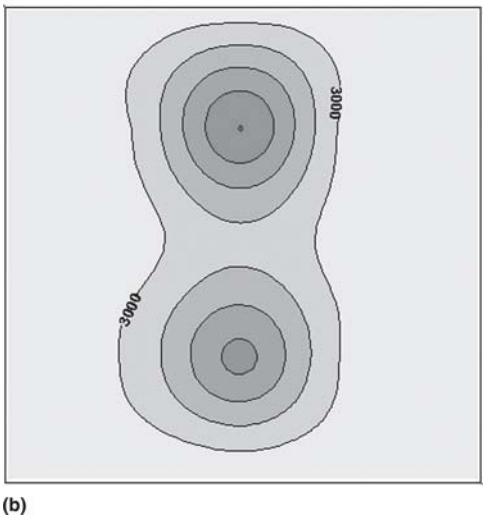


**Fig. 6** Velocity and particle flow rate contour plots in mode III (100% powder, 0% wire, 150 mm target distance)

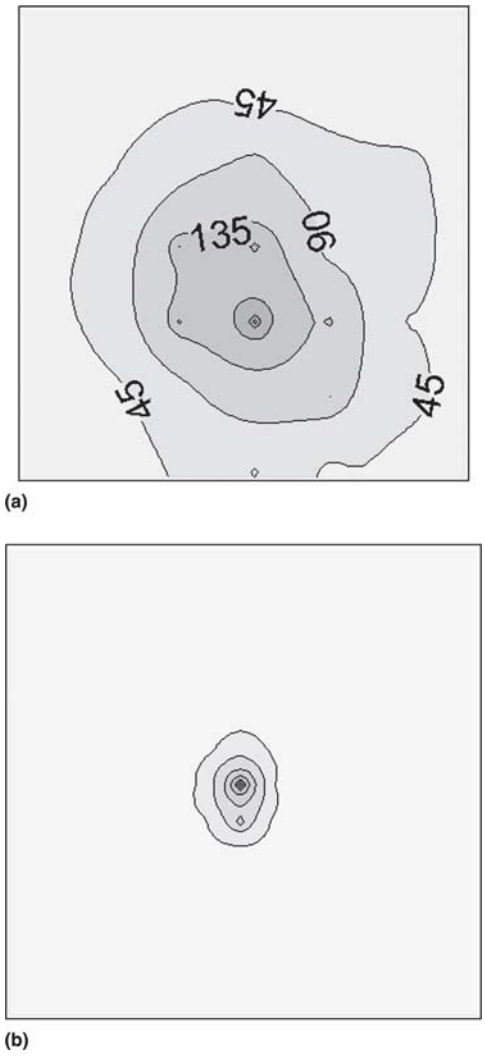


**Fig. 7** Particle flow rate contour plots in mode III: (a) single Al wire; (b) Al powder

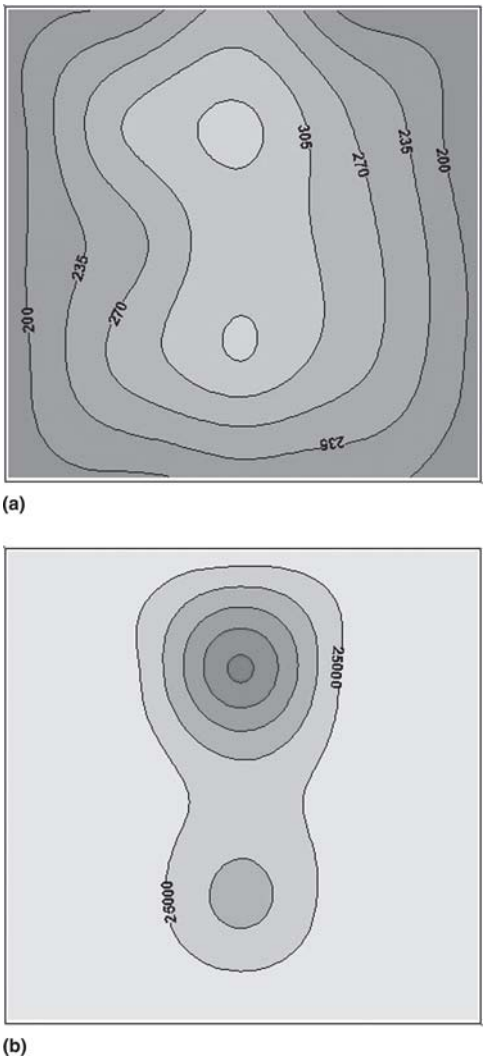


**Fig. 8** (a) Velocity and (b) particle flow rate contour plots in mode II (50% powder, 50% Ni-Al wire, 150 mm target distance)

Figure 7 presents the particle flow contour maps when the gun was operated in mode III using single Al wire and Al powder, respectively. In these experiments, the wire tips were removed from the path of the plume. As expected, the plume cross section is now different compared with Fig. 6(b). In the case of single wire (Fig. 7a), the plume was spread out more compared with the case of powder (Fig. 7b). In the case of powder, the velocity was in the range of ~400 m/s. The number of particles detected in the case of single wire was low. Also, the particle speed was slower (~200 m/s) compared with the powder feeding case. It appears that the wire melting and atomization mechanism somehow changes the particle characteristics significantly. In the case of wires, the material stays inside the jet until it melts and detaches from it. In other words, particles from the wires do not have any momentum or shape definition prior to melting. On the other hand, powders traverse through the jet and get heated, resulting in partially/fully molten particles. Therefore, the particle shape definition as well as momentum from the feeder already exists in the powders. This difference significantly contributes to the particle characteristics.

The particle velocity and flow rate contours, when the gun was switched to full-hybrid mode (mode II) running at 50% WC-16% $Cr_3C_2$-7% Ni powder and 50% Ni-Al wire, are shown in Fig. 8. The particle flow rate is higher than either mode as expected. Particle velocity is lower than in HVOF mode but is higher than in mode I. Although not greatly significant, full-hybrid mode had the greatest variation in cross-sectional plume temperature, on the order of one standard deviation. The particle mean diameter (not shown) changes very little, and a plot of the diameters resembles the mode I contour plot. The results of aluminum wire and aluminum powder combination in mode II were similar to the observations described above, except the velocity was slightly higher compared with that observed for 50% WC-16% $Cr_3C_2$-7% Ni powder and 50% Ni-Al wire.

Figure 9 illustrates the particle velocity measurements in mode II at various target distances from the gun tip. The velocity stayed constant than decreased rather than increasing and then decreasing, as in partial-hybrid mode (I), or continually decreasing, as in HVOF mode (III). However, the particle temperature remained relatively steady along the plume. The mean diameter

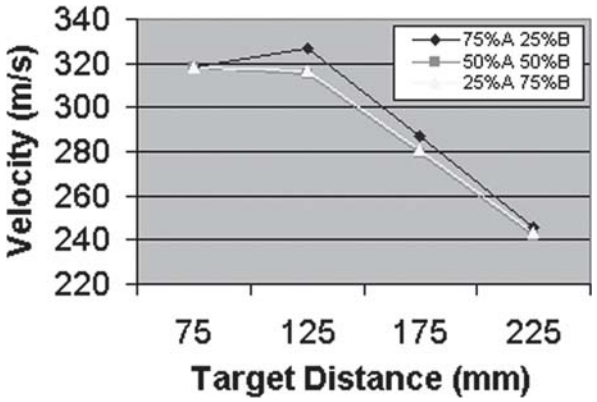


**Fig. 9** Mean particle velocity at various target distances and material combinations

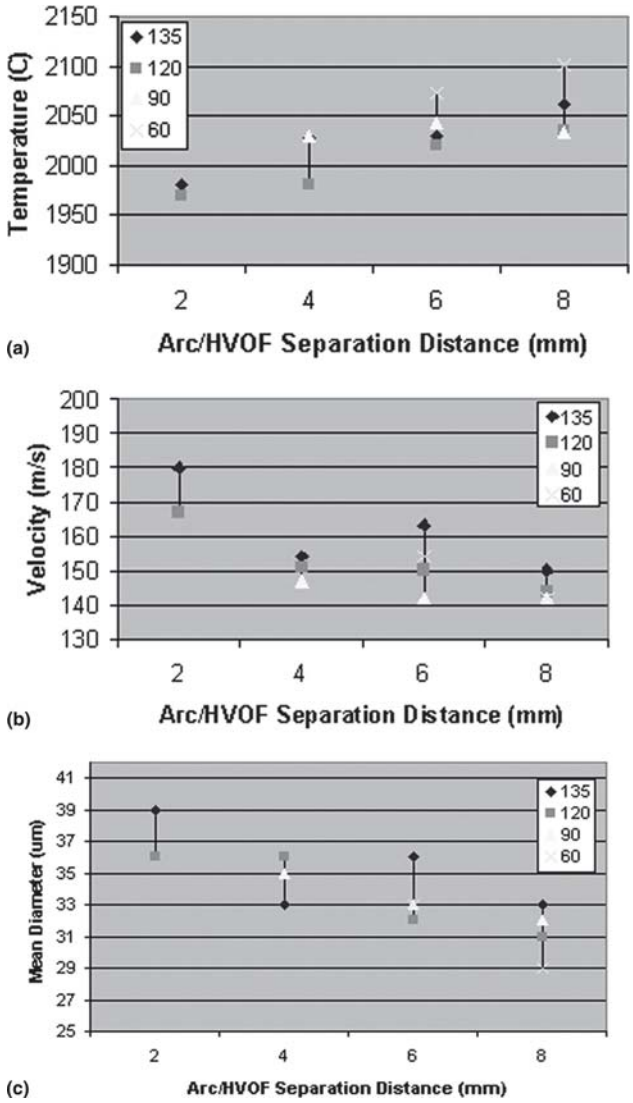


**Fig. 10** Influence of arc/HVOF separation distance in mode I at different arc-wire included angles

of detected particles in full-hybrid mode showed no significant difference along the plume. In other words, the changes in the ratio of materials did not affect the atomization characteristics of the arced material. Understandably, the feed powders are not expected to change their size, but the steady atomization behavior of the arced material is encouraging. The ratio of powder to wire did influence the particle velocity; for example, increasing the powder fraction increases the velocity in the direction of mode III operation, i.e., pure HVO mode.

It was observed that the arc-wire included angle did not have a significant influence on any particle parameter. However, the Arc/HVOF separation distance did have a noticeable effect upon all particle parameters and a considerable influence on the particle velocity. The influence of Arc/HVOF separation distance at different arc-wire included angles for Ni-Al in mode I operation is depicted in Fig. 10. The velocity and mean particle diameter decreased with increasing Arc/HVOF separation distance. However, the temperature had the opposite trend, i.e., the temperature increased with increasing separation distance.

To complement the DPV measurements and visualize the atomization phenomena, high-speed images were acquired using the camera system described earlier. Sample results in different experimental modes of the system are presented below. Figure 11 presents frames recorded at a rate of 17,500 frames/s during the operation of a conventional twin-wire arc gun using aluminum wire. The top frame was recorded to capture the arc strike point. The subsequent two frames were recorded by moving the camera focal axis 25 mm away from the previous recording position, respectively. The number and the length of the streaks observed in a frame represent the number of particles and the magnitude of their velocity, respectively. In the case of the arc gun, the acceleration rate is low as seen from these pictures. Many particles are observed to be large and move slowly in subsequent frames. The behavior of the arc/HVOF gun in mode I is shown in Fig. 12. It can be seen that the particles

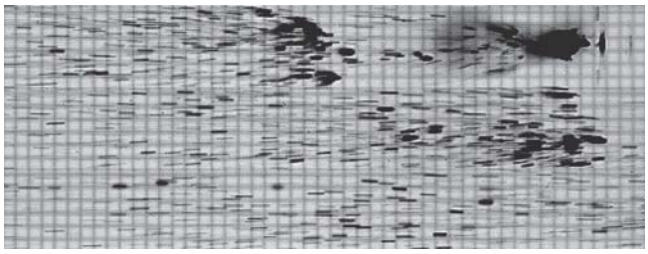

**Fig. 11** High-speed images of twin-wire arc gun with Al wire

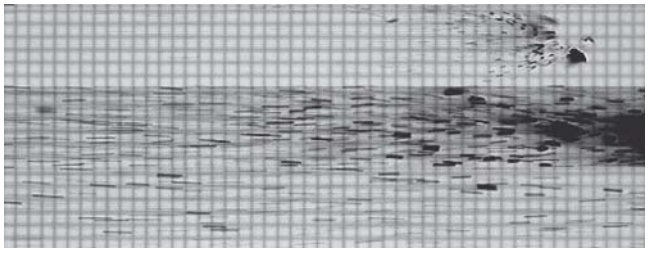

**Fig. 12** High-speed images of arc/HVOF hybrid gun in mode I operation with Al wire

velocities are much higher in this case, which is in line with DPV measurements. When Al powder was fed through the HVOF jet, the droplet speed increased further, as seen in Fig. 13, which is also in line with DPV measurements. The momentum of the incoming powders helps in the acceleration of the atomized arced metal. It is also observed that most of the particles observed in these frames were extremely fine. In other words, the impact of the powder appears to atomize the arced material efficiently.

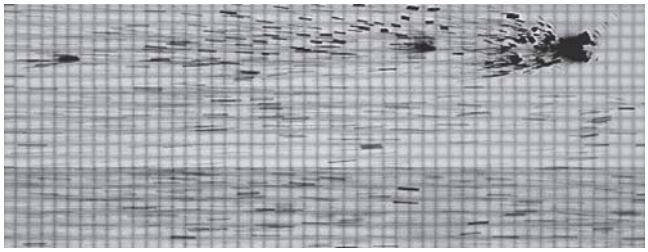

**Fig. 13** High-speed images of arc/HVOF hybrid gun in mode II operation with Al wire and Al powder

Figure 14(a) presents atomization behavior of two wires by the HVOF jet only, i.e., no potential was maintained across the wires. Both the wires melted and atomized independently. The corresponding particle flow rate contour plot is shown in Fig. 14(b). Note that the plume cross sections were measured 25 mm away from the arcing point. The atomization behavior of the wires in the presence of a potential is shown in Fig. 15(a). Here, a gap was maintained such that the wires would not strike an arc automatically. When the combustion jet was ignited, an arc was established through the flame and melted wire, steadily delivering a plume. The corresponding plume cross-section map is shown in Fig. 15(b). It is observed that the plume is tighter compared with the case of no potential and no arc. Because it is a plasma, the combustion jet is expected to have good conductiv-

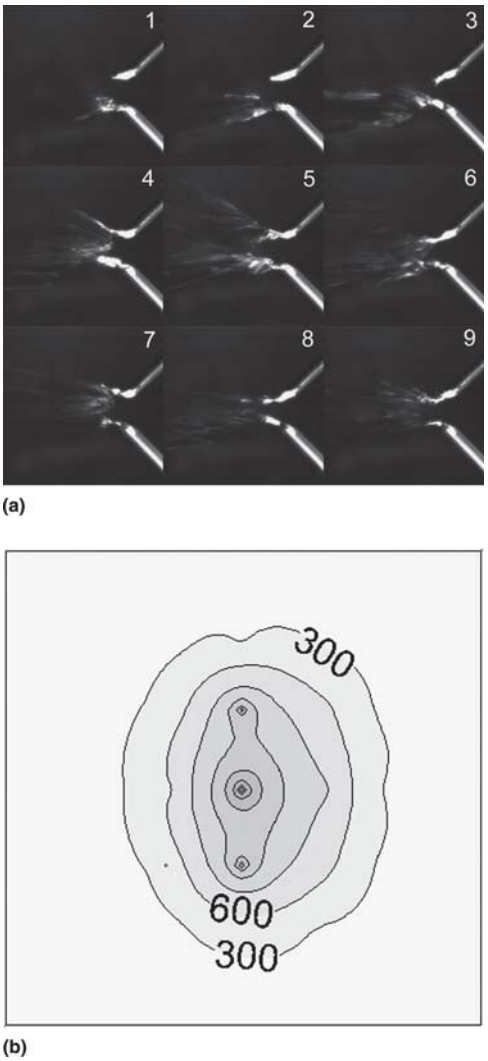


**Fig. 14** (a) High-speed images of hybrid gun with no potential or arcing and (b) particle flow rate contour plots of hybrid gun with no potential or arcing

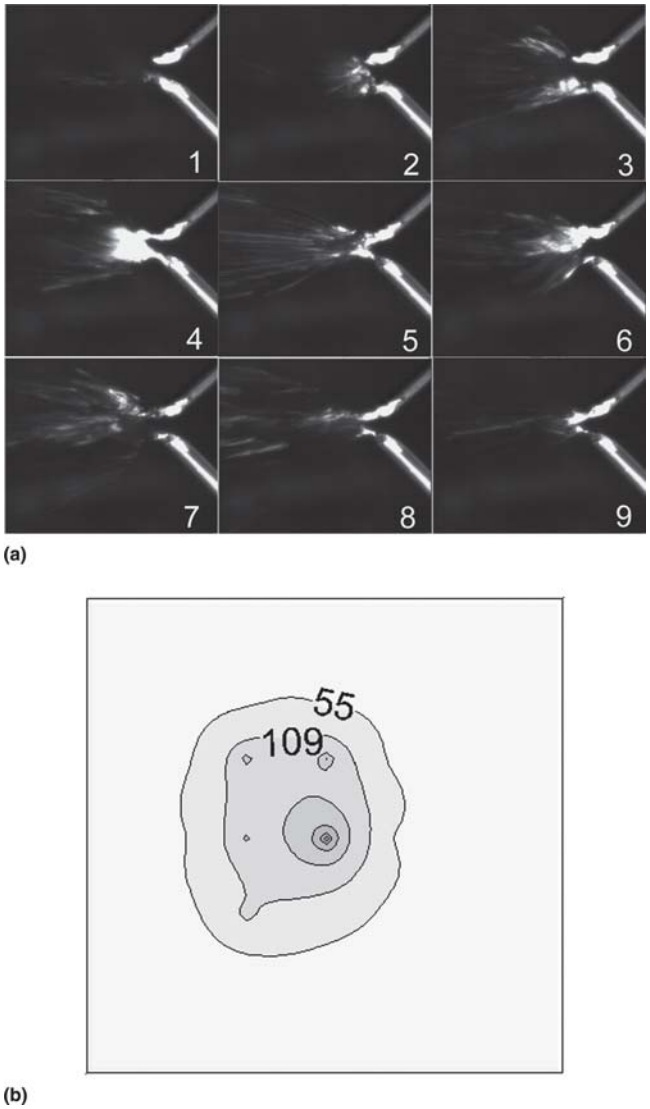


**Fig. 15** (a) High-speed images of hybrid gun with potential but not arcing and (b) particle flow rate contour plots of hybrid gun with potential but not arcing

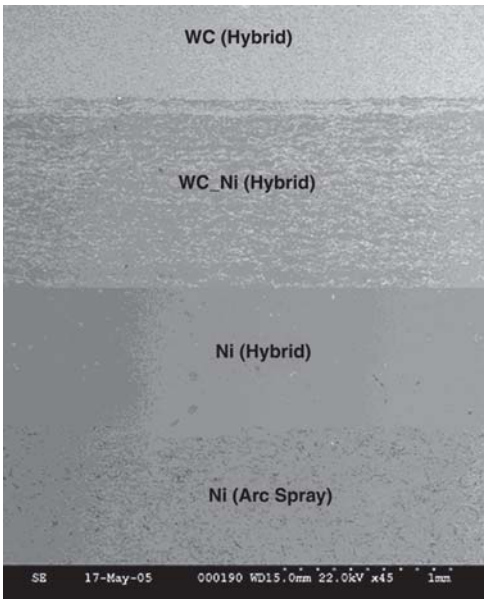


**Fig. 16** Comparison of coatings made by the hybrid gun and arc-spray gun

ity. The molten metal also establishes the conduction path between the wires. As a result, the arc can be maintained at low amperage.

The different operational modes and their influence on the coating quality is an interesting topic, but these are beyond the scope of the present paper. A sample single coating obtained with various modes of the gun as well as a coating from a conventional arc-spray gun are presented in Fig. 16. The capability and quality of the coating obtained by hybrid gun are self-evident. Compared with the arc-sprayed coating, the hybrid gun coating is very dense and the types of coatings that can be produced from the hybrid gun are very unique.

## 4. Summary

This paper described diagnostic experiments on a hybrid HVOF arc-spray gun using a DPV diagnostic system as well as high-speed imaging. The following observations were made:

- Particle velocity of the arced metal was significantly higher than that from a conventional electric wire arc gun. The particle size was quite uniform and small. This results in high coating density, which has been observed in this process for different materials. Particle temperatures remained steady in the entire plume.
- Spray particle velocity was strongly dependent on the mode of operation. In HVOF mode, particle velocities up to 400 m/s were observed. This is slightly low compared with the commercial HVOF guns. In full-hybrid mode, the particles had intermediate velocities. The arc angle did not influence the particle velocity or the temperature. However, the arc/HVOF separation distance had a significant influence on particle velocity.
- High-speed images agreed well with the general observations made by the DPV system. For example, the speed of arced droplets is augmented when powder particles are injected through the jet. The atomization process in the arc/HVOF gun was steadier compared with that of the twin-wire arc gun. Even if the wires were not touching, arc struck through the flame in the hybrid gun.

Although there are some limitations, such as particle detectability and large standard deviations, the diagnostic systems described here successfully characterize the ensemble average characteristics of the spray plume. For processes such as FGM fabrication, the ensemble average characteristics are very useful for parameter selection and will lead to a better quality deposit.

### Acknowledgment

Financial support from the U.S. Army-TARDEC, under contract number DAAE07-03-C-L148, is gratefully acknowledged.

### References

1. D. Kosikowski, M. Batalov, and P.S. Mohanty, Functionally Graded Coatings by HVOF-Arc Hybrid Spray Gun, *Thermal Spray 2005,* May 2-4, 2005 (Basel, Switzerland), ASM International, 2005, p 444-449
2. D. Kosikowski, M. Batalov, and P. Mohanty, In-Flight Particle Characterization of HVOF-Arc Hybrid Gun, *Thermal Spray 2005,* May 2-4, 2005 (Basel, Switzerland), ASM International, 2005, p 785-790
3. A. Vaidya, T. Streibl, L. Li, S. Sampath, O. Kovarik, and R. Greenlaw, An Integrated Study of Thermal Spray Process-Structure-Property Correlations: A Case Study for Plasma Sprayed Molybdenum Coatings, *Mater. Sci. Eng. A,* 2005, **403**(1-2), p 191-204
4. S. Guessasma, G. Montavon, and C. Coddet, Velocity and Temperature Distributions of Alumina-Titania In-Flight Particles in the Atmospheric Plasma Spray Process, *Surf. Coat. Technol.,* 2005, **192,** p 70-76
5. M. Cherigui, Z. Salhi, N.E. Fenineche, P. Gougeon, and C. Coddet, FeSi HVOF Thermal Spray Coatings: Diagnostic, Microstructure, and Magnetic Properties, *Mater. Lett.,* 2005, **59**(4), p 463-467
6. Z. Salhi, P. Gougeon, D. Klein, and C. Coddet, Influence of Plasma Light Scattered by In-Flight Particle on the Measured Temperature by High Speed Pyrometry, *Infrared Phys. Technol.,* 2005, **46**(5), p 394-399
7. Z. Salhi, S. Guessasma, P. Gougeon, D. Klein, and C. Coddet, Diagnostic of YSZ In-Flight Particle Characteristics under Low Pressure VPS Conditions, *Aero. Sci. Technol.,* 2005, **9**(3), p 203-209
8. M. Li, D. Shi, and P.D. Christofides, Model-Based Estimation and Control of Particle Velocity and Melting in HVOF Thermal Spray, *Chem. Eng. Sci.,* 2004, **59**(22-23), p 5647-5656
9. J.R. Fincke, W.D. Swank, R.L. Bewley, D.C. Haggard, M. Gevelber, and D. Wroblewski, Diagnostics and Control in the Thermal Spray Process, *Surf. Coat. Technol.,* 2001, **146-147,** p 537-543
10. C.M. Hacket and G.S. Settles, Independent Control of HVOF Particle Velocity and Temperature, *Thermal Spray: Practical Solutions for Engineering Problems,* Oct 7-11, 1996 (Cincinnati, OH), C.C. Berndt, Ed., ASM International, 1996, p 665-673
11. W. Lih, S.H. Yang, C.Y. Su, S.C. Huang, I.C. Hsu, and M.S. Leu, Effects of Process Parameters on Molten Particle Speed and Surface Temperature and the Properties of HVOF CrC/NiCr Coatings, *Surf. Coat. Technol.,* 2000, **133-134,** p 54-60
12. S. Guessasma, Z. Salhi, G. Montavon, P. Gougeon, and C. Coddet, Artificial Intelligence Implementation in the APS Process Diagnostic, *Mater. Sci. Eng. B,* 2004, **110**(3), p 285-295
13. W.L.T. Chen, J. Heberlein, and E. Pfender, Diagnostics of a Thermal Plasma Jet by Optical Emission Spectroscopy and Enthalpy Probe Measurements, *Plasma Chem. Plasma Proc.,* **14**(3), 1994, p 317-332
14. M. Asmann, A. Wank, H. Kim, and J. Heberlein, Characterization of the Converging Jet Region in a Triple Torch Plasma Reactor, *Plasma Chem. Plasma Proc.,* 2001, **21,** p 37-63
15. L. Duan and J. Heberlein, Arc Instabilities in a Plasma Spray Torch, *J. Therm. Spray Technol.,* 2002, **11**(1), p 44-51

16. L. Duan, J. Beall, J. Schein, J. Heberlein, and M. Stachowicz, Diagnostics and Modeling of an Argon/Helium Plasma Spray Process, *J. Therm. Spray Technol.,* 2000, **9,** p 225-234
17. P.S. Mohanty, R. Allor, P. Lechowicz, R. Parker, and J. Craig, Particle Temperature and Velocity Characterization in Spray Tooling Process by Thermal Imaging Technique, *Thermal Spray 2003: Advancing the Science and Applying the Technology,* May 5-8, 2003 (Orlando, FL), B.R. Marple and C. Moreau, Ed., ASM International, 2003, Vol 2, p 1183-1190
18. M. Cetegen and W. Yu, In-Situ Particle Temperature, Velocity, and Size Measurements in DC Arc Plasma Thermal Sprays, *J. Thermal Spray Technol.,* 1999, **8**(1), p 57-67
19. K. Hollis and R. Neiser, Particle Temperature and Flux Measurement Utilizing a Nonthermal Signal Correction Process, *J. Thermal Spray Technol.,* **7**(3), 1998, p 392-402
20. J.R. Fincke, C.L. Jeffery, and S.B. Englert, In-Flight Measurement of Particle Size and Temperature, *J. Phys. E: Sci. Instrum,* 1988, **21,** p 367-370
21. A. Cezairliyan, S. Krishnan, and J.L. McClure, Simultaneous Measurements of Normal Spectral Emissivity by Spectral Radiometry and Laser Polarimetry at High Temperatures in Millisecond-Resolution Pulse-Heating Experiments, *Int. J. Thermophys.,* 1999, **17**(6), p 1455-1473
22. J.R. Fincke and R.A. Neiser, Advanced Diagnostics and Modeling of Spray Processes, *MRS Bull. Mater. Res. Soc.,* 2000, **25**(7), p 26-31
23. S.P. Mates, D. Basak, F.S. Biancaniello, S.D. Ridder, and J. Geist, Calibration of a Two-Color Imaging Pyrometer and Its Use for Particle Measurements in Controlled Air Plasma Spray Experiments, *J. Thermal Spray Technol.,* 2002, **11**(2), p 195-205
24. J.R. Fincke, D.C. Haggard, and W.D. Swank, Particle Temperature Measurement in the Thermal Spray Process, *J. Thermal Spray Technol.,* 2001, **10**(2), p 255-266
25. J. Vattulainen, E. Hämäläinen, R. Hernberg, P. Vuoristo, and T. Mäntylä, Novel Method for In-Flight Particle Temperature and Velocity Measurements in Plasma Spraying Using a Single CCD Camera, *J. Thermal Spray Technol.,* 2001, **10**(1), p 94-104
26. M.P. Planche, H. Liao, B. Normand, and C. Coddet, Relationships between NiCrBSi Particle Characteristics and Corresponding Coating Properties Using Different Thermal Spraying Processes, *Surf. Coat. Technol.,* 2005, **200**(7), p 2465-2473
27. M.P. Planche, H. Liao, and C. Coddet, Relationships between In-Flight Particle Characteristics and Coating Microstructure with a Twin Wire Arc Spray Process and Different Working Conditions, *Surf. Coat. Technol.,* 2004, **182**(2-3), p 215-226
28. T. Watanabe, T. Sato, and A. Nezu, Electrode Phenomena Investigation of Wire Arc Spraying for Preparation of Ti-Al Intermetallic Compounds, *Thin Solid Films,* 2002, **407**(1-2), p 98-103
29. T. Watanabe, X. Wang, E. Pfender, and J. Heberlein, Correlations between Electrode Phenomena and Coating Properties in Wire Arc Spraying, *Thin Solid Films,* 1998, **316**(1-2), p 169-173